Archives of Materials Science and Engineering

Volume 110
Issue 1
July 2021
Pages 5-17

International Scientific Journal
published monthly by the
World Academy of Materials
and Manufacturing Engineering

DOI: 10.5604/01.3001.0015.3591

Gas hydrates impact on corrosion of the well flow lines material

L. Poberezhny [a], A. Hrytsanchyk [b], O. Mandryk [c], L. Poberezhna [c], P. Popovych [d], O. Shevchuk [d], B. Mishchuk [b], Yu. Rudyak [e]

[a] Department of Chemistry, Institute of Tourism and Geosciences, Ivano-Frankivsk National Technical University of Oil and Gas, 15, Karpatska str., Ivano-Frankivsk, Ukraine
[b] Department of Petroleum Production, Institute of Petroleum Engineering, Ivano-Frankivsk National Technical University of Oil and Gas, Ivano-Frankivsk, Ukraine
[c] Department of Ecology, Institute of Tourism and Geosciences, Ivano-Frankivsk National Technical University of Oil and Gas, Ivano-Frankivsk, Ukraine
[d] Department of Specialized Computer Systems, West Ukrainian National University, 11 Lvivska Str., Ternopil, Ukraine
[e] I. Horbachevsky Ternopil National Medical University, Ternopil, Ukraine
* Corresponding e-mail address: lubomyrpoberezhny@gmail.com
ORCID identifier: https://orcid.org/0000-0001-6197-1060 (L.P.); https://orcid.org/0000-0001-9894-0911 (A.H.); https://orcid.org/0000-0002-2689-7165 (O.M.); https://orcid.org/0000-0002-4944-0192 (L.P.); https://orcid.org/0000-0001-5516-852X (P.P.); https://orcid.org/0000-0001-6453-355X (O.S.); https://orcid.org/0000-0003-1836-9132 (Yu.R.)

ABSTRACT

Purpose: Determination of regularities of joint action of mechanical stresses, formation water and hydrate formation on corrosion of material of flow pipelines.

Design/methodology/approach: According to the analysis of reservoir water of the investigated deposits, it was found that the main corrosive component is soluble chlorides. Proposed for corrosion and corrosion-mechanical tests of 6 model environments. An estimation of the influence of stress concentration, depending on the defects of the inner wall of the pipe, was carried out, and the nominal local stresses in the pipeline was carried.

Findings: The basic regularities of influence of stress and hydration formation on corrosion and localization of corrosion processes and on the kinetics of deformation of samples are described. For samples made of steel 20 and 17GS, an increase in the velocity of general and local corrosion for samples sustained in the gas hydrate was observed compared to the control results obtained, the coefficient of influence of the gas hydrate on corrosion was calculated.

Research limitations/implications: The obtained results are valid for thermobaric operating conditions of well flow lines.

Practical implications: The data obtained in the work on the patterns of corrosion processes and the impact of hydrate formation on them will allow to identify potentially dangerous areas of flow lines and prevent emergencies.

Originality/value: Based on the analysis of the geometric dimensions of the defects, the effective stress concentration coefficients are calculated, and it is shown that the stresses in the vicinity of corrosion defects in normal operating modes range from 164 to 545 MPa.

Keywords: Gas hydrate, Oil and gas region, Corrosion-mechanical tests, Influence of hydrate formation, Inner pipe corrosion

Reference to this paper should be given in the following way:

L. Poberezhny, A. Hrytsanchyk, O. Mandryk, L. Poberezhna, P. Popovych, O. Shevchuk, B. Mishchuk, Yu. Rudyak, Gas hydrates impact on corrosion of the well flow lines material, Archives of Materials Science and Engineering 110/1 (2021) 5-17.

DOI: https://doi.org/10.5604/01.3001.0015.3591

PROPERTIES

1. Introduction

Along with the development of the oil and gas industry, it is necessary to solve environmental problems, as soil, water, air, which are direct factors in the technological process, undergo adverse transformation, and only reducing or eliminating the negative effects ensures environmental and economic safety [1-5].

Hydrates can initiate certain types of internal corrosion of gas pipelines. This problem is multifaceted due to physical and chemical processes, which depend on the size of the formed hydrate, the stage and period of its contact with the pipeline, as a result of which the destruction of protective films on the surface. Acid gases, in particular H_2S, CO_2, which are components in the formation of gas hydrates, as well as Cl^- ions, interacting with water contribute to the acceleration of internal corrosion of gas pipelines. At each stage of the hydrate formation process, there is a chemical interaction between the hydrate components and the metal of the pipeline, which initiates the beginning of internal corrosion, which in turn will lead to gradual degradation of the material and deterioration of the integrity of the pipe. The pipeline will start to leak and this can provoke a full breakage. This prospect can cause economic, environmental and political consequences, as well as lead to the replacement of pipes along the entire length of the pipeline and additional production costs [5-7].

In most cases, formation waters have a pH close to neutral. pipes of emission lines of drilling do not have electrochemical protection, corrosion defeats of an internal surface of pipes have the expressed localization. Because carbon and low-alloy steels are used for the discharge lines, no cases of stress-corrosion cracking were observed [1-7]. Clogging with gas hydrates of industrial gas pipelines in the autumn-winter period is always accompanied by favourable thermodynamic environmental conditions [8-9], high pressure and low temperature of transportation [10-13]. Therefore, the urgent task is to analyse the causes of emergencies due to the formation of gas hydrates, in particular inner-pipe corrosion, and to establish patterns of influence of gas hydrates on the physical and mechanical characteristics of the pipeline material. This will make it possible to develop science-based engineering solutions to overcome the problems of the gas industry related to gas hydrate formations [6-8].

2. Materials and methods

For structures of the oil and gas industry, the cyclic loading is carried out at stresses below the yield strength of the material. In this case, the presence of stress concentration leads to a strong increase in local stresses of the cycle, the level of which determines the fatigue life of the pipeline [14-20].

Theoretical and experimental studies show that in the area of a sharp change in the shape of the elastic body (concentrator), i.e. in the presence of mechanical damage (cavities, cracks, leaks, corrosion damage), there are increased stresses. The appearance of the inner surface of the pipeline is shown in Figures 1 and 2 The presence of stress concentrators significantly affects the process of fatigue failure [19, 21-23].

Fig. 1. General view of the inner wall of the pipe

Fig. 2. Profilogram of the inner wall of the flow line

The quantitative characteristic of the stress concentration is the theoretical stress concentration factor α_σ [24].

$$\alpha_\sigma = \frac{\sigma_{max}}{\sigma_{nom}} \quad (1)$$

where σ_{max} – the greatest local stress; σ_{nom} – nominal stress.

To assess the effect of concentration on the strength of the material, an effective concentration factor is introduced K_σ, which is equal to the ratio of the destructive load of the sample without a concentrator to the destructive load of the sample with the same cross section with the stress concentrator.

$$K_\sigma = \frac{\sigma_{-1}}{\sigma_{-1k}}, \quad (2)$$

where σ_{-1} – endurance limit of samples without stress concentration, a σ_{-1k} – endurance limit of samples with stress concentration, which are calculated as nominal stresses for a smooth sample with the same cross section.

For an approximate calculation of the effective concentration factor, $K_\sigma$use [21] to obtain:

$$K_\sigma = 1 + q_\sigma(\alpha_\sigma - 1), \quad (3)$$

where q_σ is the coefficient of sensitivity to stress concentration, for St20 steel $q_\sigma = 0.75$.

To calculate the theoretical concentration coefficient, we use the dependences that depend on the length (c), width (d) and depth (b) [21,25].

Simplified dependence for calculation of theoretical concentration coefficient.

$$\alpha_\sigma = 1 + 2 \cdot \frac{a}{b}, \quad (4)$$

where *a, b* – respectively, the half-axis of the elliptical defect.

For a separate cavity (hole-shaped sink) it is recommended to use the formula:

$$\alpha_\sigma = 1 + 3.75 \cdot \frac{b}{d} \cdot \frac{1.12 - 0.9 \cdot \frac{b}{c}}{1 - \frac{b}{h \cdot \left(1 - 1.5 \cdot \left(\frac{b}{c}\right)\right)}} \quad (5)$$

For mechanical damage such as dents and conditions $0{,}1 \le d/D \le 0{,}3$ and $0 \le b/\delta \le 2$, D – outer diameter of the pipeline, m; δ – average wall thickness, m.

$$\alpha_\sigma = 1 + 2 \cdot \frac{b}{h} + 0.475 \cdot \left(\frac{b}{d}\right)^2 - \frac{b}{D} \cdot \left(5 - \frac{b}{h} - 0.75 \cdot \left(\frac{b}{h}\right)^2\right) \quad (6)$$

The main results calculated by formulas (3-6) are presented in Table 1, indicating the geometric dimensions of the corresponding corrosion defects.

From the data of Table 1 it follows that the effective concentration factor for different types of caverns significantly depends on their shape. Thus, the total stress in the inner wall of the damaged pipeline will be 1.243-4.595 times higher for the defect with large longitudinal dimensions and small depth and the defect with large depth of damage, respectively, which allows us to say with confidence about the significant negative impact of local corrosion.

To establish stresses in the vicinity of the corrosion defect of oil and gas regions with the highest potential risks of hydrate formation, the average operational data for each region were used separately. It is established that the highest operational pressures and thus the highest stress values in the vicinity of the corrosion defect are observed in the Hlynsko-Solokhiv oil and gas region (Tab. 2).

Therefore, from the obtained results of calculation of stress concentration coefficients it follows that the stresses in the defective pipe are several times higher than the nominal ones, which indicates the need to increase the range of load levels for mechanical and corrosion-mechanical tests [26,27]. Based on the calculations, the stress range for mechanical tests 240-510 MPa was selected. A detailed analysis of the composition of water extracted from wells in the oil and gas regions of Ukraine showed that they belong

Table 1.
The results of the calculation of the effective concentration ratio

Dimensions of the defect			Theoretical concentration factor			Effective concentration factor		
c, mm	d, mm	b, mm	by formula (4)	by formula (5)	by formula (6)	by formula (4)	by formula (5)	by formula (6)
3.837	3.439	1.348	2.793	2.55	1.598	2.344	2.162	1.523
3.407	1.786	1.191	2.048	3.545	1.71	1.786	2.909	1.607
18.19	9.525	0.711	2.047	1.324	1.421	1.785	1.243	1.391
14.354	10.517	1.158	2.465	1.486	1.499	2.099	1.364	1.449
13.758	4.366	1.455	1.635	2.496	1.595	1.476	2.122	1.521
4.696	1.389	1.25	1.592	4.595	1.893	1.444	3.696	1.745
6.747	6.218	1.235	2.843	1.829	1.525	2.382	1.622	1.468

mainly to the hydrocarbonate and calcium chloride type with a total mineralization of 1.2-300 g/l, a density of about 1.0-1.09 g/cm^3 and acidity pH = 5.2-7.7. The high degree of metamorphosis – more than 0.87 indicates the absence of water exchange zones and the closedness of the hydrogeological basin.

The most common corrosive components in the formation waters of the experimental region are chlorine ions, the content of which ranges from 10 to 250 g/l. The average chemical composition of the studied formation waters (Tab. 3) showed a large variation in the content of chlorides and to a lesser extent sulfates [28]. The content of chloride ions is taken to create solutions of model media, which are used in corrosion and corrosion-mechanical tests. The concentration of chlorides in reservoir water samples ranges from 593.4 to 94799 mg/l, which formed the basis of the formulation of the choice of the chemical composition of the model media.

Table 2.
Stress in the corrosion defects in normal operation

Oil and gas region	Working pressure maximum average, MPa	Stress in the pipeline wall maximum average, MPa	Stress in corrosion defect, maximum average, MPa
Mashivsko-Shebelinsky	9.8 4.8	141.2 132.1	175.5–521.8 164.1–488.0
Hlynsko-Solokhivsky	12.8 8.1	147.9 137.8	183.8–546.5 171.3–509.3
Pivnichnoho Bortu	7.0 5.4	135.7 133.0	168.7–501.7 165.3–491.6
Bilche-Volytsky	3.9 2.1	130.7 128.3	161.3–483.1 157.9–474.2

Table 3.
Ion concentration in produced waters in main oil and gas production regions of Ukraine

Region	Test point	Ion concentration, mg/l					
		Na^++K^+	Ca^+	Mg^{2+}	Cl^-	SO_4^{2-}	HCO_3^-
1	2	3	4	5	6	7	8
Bilche-Volytsky	1	17784.14	1603.2	732	32006.8	72.44	640.5
	2	17197.24	1683.36	683.2	30963.0	18.11	945.5
	3	24064.60	1683.36	622.2	41748.0	14.82	335.5
	4	14758.16	981.96	561.2	25396.7	100.02	1189.5
	5	40574.07	5210	1216	74466	1081.16	97.6
	6	29098	5094	722	55884	320	244
Hlynsko-Solokhivsky	1	29420	4788	1267	57243	334	549
	2	38912	5968.04	481.20	18105.00	512.6	658.8
	3	593.4	10220	240	19525	182	122
	4	67693.12	24562.83	2403.44	156234.6	31.27	176.9
	5	64564.77	13327.4	5733.28	139370.22	555.55	115.9
	6	8528.63	2005.00	364.8	17750.	9.87	36.6
	7	760.61	67568.5	1216	124250.0	70.76	97.6
	8	5533.80	1203.02	486.4	17070	-	6.6
Pivnichnoho bortu	1	18424.61	2807.0	729.6	35500.0	13.16	48.8
	2	50030.29	12024	3952	109704.38	2304	366
	3	47503.97	11022	1520	96539.85	205.75	827.06
	4	48594.4	10172.3	1913.45	96074.00	1608.14	2135
	5	40685	6971	1933	80475	216	46.1
	6	46798	6821	3173	97738	962	56.1
	7	45502	47094	5776	166946	221	230

Region	Test point	Ion concentration, mg/l					
		$Na^+ + K^+$	Ca^+	Mg^{2+}	Cl^-	SO_4^{2-}	HCO_3^-
1	2	3	4	5	6	7	8
Talalaivsko-Rybalsky	1	47336	35571	4256	148046	215	220
	2	61159	20391	760	151977	592	214
	3	64674	16171	4269	140342	505	525
	4	1337.6	1604	18683.0	35500	6.58	134.2
	5	1094.40	7214.4	19196.7	45388.8	107.8	146.6
	6	40684.3	1032.38	5954.69	75301.1	513.55	597.8
Rudenkivsko-Proletarsky	1	40845.4	1193.63	6539.4	77927.9	376.93	237.9
	2	26290.4	972.8	3206.4	48934.8	98.76	61.01
	3	36352.4	-	5410.8	65601	11.52	18.3
	4	26748.3	729.6	3607.2	49644	65.84	97.62
	5	28004.8	790.4	3406.8	51414	57.61	85.41
	6	61738.9	6972.9	4749.12	124110	1211.87	170.8
Mashivsko-Shebelinsky	1	31761.8	10020	3344	76239	9.87	366
	2	41480.51	2699.99	2730.53	71874.6	4649.95	1403
	3	8588.2	2805	1840	20590	86.4	97.6
	4	13751.7	7615	1440	98695	168	2684
	5	9526.6	3206	960	23075	86.4	146.4
	6	28155.68	4959.9	1094.4	54888.91	22056	561.2
	7	72356.16	54430	4444.44	169361.28	-	268.4
	8	61202.08	6729.11	3883.36	118200.06	646.88	640.5
	9	77964.98	8050.07	1186.68	137063.79	522.6	292.8

Table 4.
The chemical composition tested steels

Material	Elements, %						
	C	Si	Mn	Ni	S	P	Cr
17GS steel	0.14-0.20	0.40-0.60	1.00-1.40	≤0.30	≤0.035	≤0.030	≤0.30
St20 steel	0.17- 0.24	≤0.07	0.25- 0.50	≤0.30	≤0,040	≤0.035	≤0.25

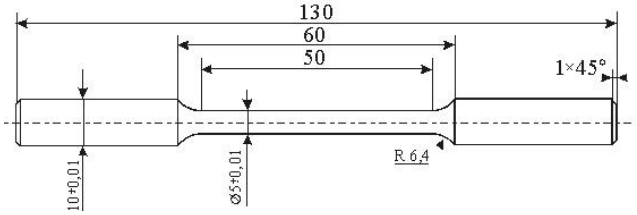

Fig. 3. Design of samples for testing

The object of the study was selected industrial pipelines made of steel 20 and 17GS (Tab. 4). According to the developed methodology.

At the first stage, model samples are made (Fig. 3) from the material of certain sections of the pipeline, or individual pipes, in order to effectively use the theory of structural similarity;

On the second – load schemes and test modes are selected in order to achieve on the samples-models, with a predetermined configuration, simulation of the work of the investigated material in the structure;

At the third stage, the experimental samples are laid in the reactor and the synthesis of gas hydrates (Fig. 4).

There are several schemes for the formation of gas hydrates:

I. Scheme without mechanical oscillations of the reactor:
   1. The sample is fixed in the holes of the rings made of plexiglass (Fig. 5) the location of the samples is shown in Figure 6.
   2. The frame is installed in the reactor (Fig. 6).

II. Scheme with the action of mechanical oscillations of the reactor. This scheme is similar to scheme 1 only after the formation of hydrate on the surface of the sample (Fig. 7) additionally turns on the generator of mechanical

oscillations of the reactor. This test method makes it possible to better assess the effect of hydrate in the presence of a large amount of domestic water in conditions of significant turbulence of the gas-water flow.

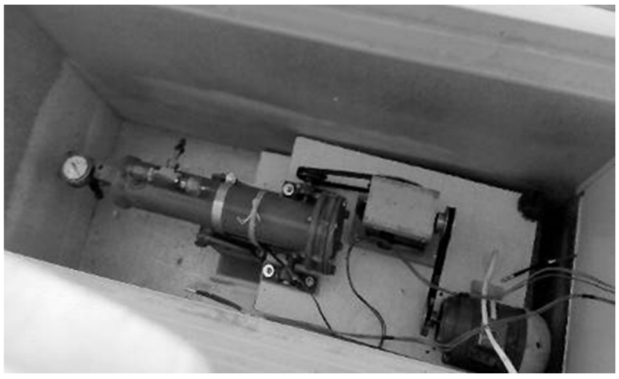

a)

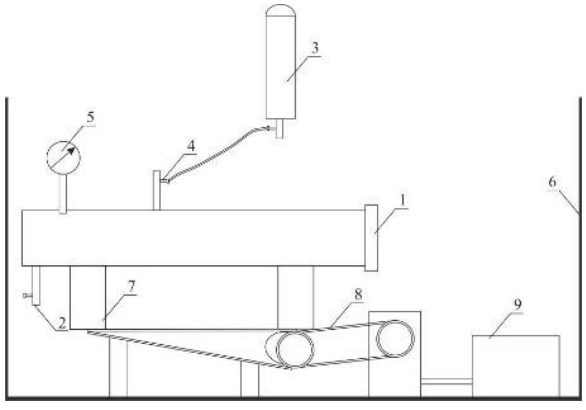

b)

Fig. 4. General view (a) and scheme (b) of the installation for the synthesis of gas hydrates. 1 – experimental reactor, 2 – drain pipe, 3 – gas cylinder, 4 – inlet pipe, 5 – manometer, 6 – refrigerator, 7 – support, 8 – belt drive, 9 – electric motor

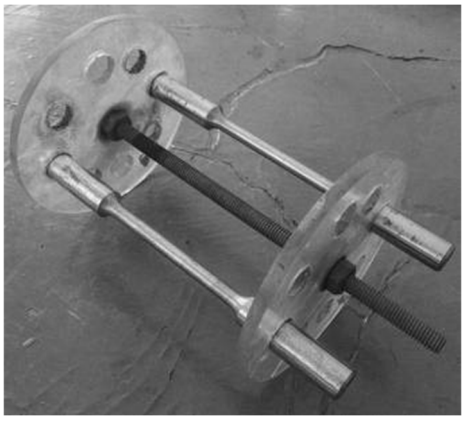

Fig. 5. General view of the frame for mounting samples in the reactor

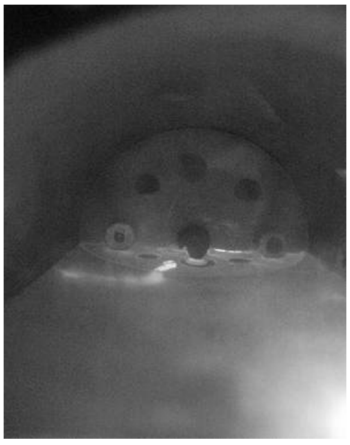

Fig. 6. Location of model samples in the middle of the reactor according to the scheme in which the samples are above the level under the commercial water

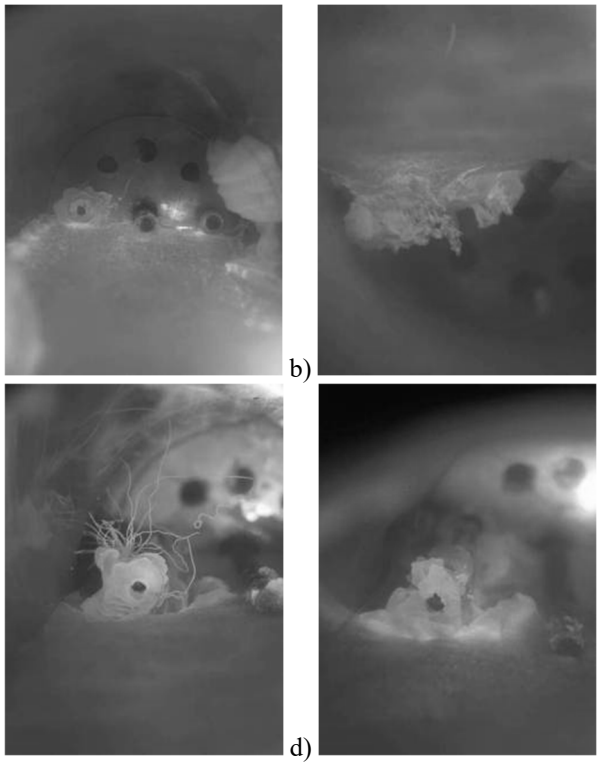

a) b) c) d)

Fig. 7. Artificial gas hydrate on the surface of the sample in the gas part (a, c, d) and in the liquid (b)

This scheme provides for the installation of samples in any order in the frame, because after the formation of lumps of hydrate and the inclusion of the generator of mechanical vibrations, the effect on all samples-models will be on the entire plane of the frame.

The process of laying the studied samples-models in the rector for the synthesis of gas hydrates is carried out in the following sequence:

- disconnect the end part of the reactor 1, which provides access to the middle of the reactor;
- close the drain valve 2;
- in the reactor through its end with flanges, fresh water in volume is filled in 1 l;
- immerse in the reactor test specimens mounted on the frame, which prevents their distortion during the research;
- close the end of the reactor with a metal ring with a hole between which is placed plexiglass thick 3 cm to observe the formation of gas hydrate crystals;
- by means of a gas compressor 3 is pumped through the valve 4 gas - methane, until the pressure in the system at the level of 45 atm, as indicated by the manometer 5;
- in the refrigeration unit 6 a temperature of 2.5°C is created;
- the reactor is mounted on supports 7 in the middle of the refrigeration unit;
- for circuit 2 it is necessary to turn on the engine 9, which through the belt drive 8 will cause the reactor to oscillating motion;
- samples of pipeline material are kept in the reactor at a certain exposure time.

There are several schemes for establishing a sample model in the reactor relative to the liquid level (Fig. 8).

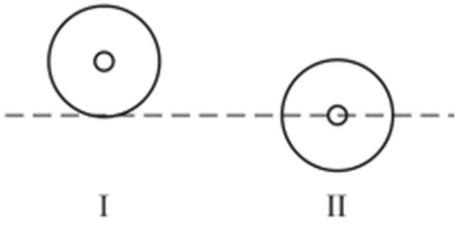

Fig. 8. Sample installation schemes: the sample above the water level (I), the middle of the sample is at the gas-water phase separation (II)

Table 5.
Chemical composition of the studied formation waters

Model environment	NaCl concentration, mol/l
1	0.5
2	1.5
3	2.5
4	3.75
5	5

Chemical composition of the studied formation waters is shown in Table 5. For each combination of "mechanical stress – chloride concentration" was tested 3 samples. Time of exposition in corrosive environment – 7 days (168 hours).

3. Results and discussions

According to the results of studying the corroded surfaces of the samples aged in gas hydrate, the mechanism of its influence on the corrosion of the pipeline material is only intensifies and localizes the effect of corrosive components of formation waters. In the first stage (the stage of hydrate formation) the surface of the metal around it continues to be covered with passive films of corrosion products, while on the surface of the metal under the hydrate this process stops.

In addition, as a result of the formation of hydrate crystals due to moisture, which is adsorbed by the corrosion products, there is a partial destruction of the passive film, because the volume of the formed crystals is 2-3 times larger than the volume of water. After dissociation of the hydrate (stage 2), a potential difference is formed between the described parts of the metal, which causes corrosive microgalvanic elements that accelerate the dissolution of the metal in a less passive zone. In the future, when thermobaric conditions favourable for hydrate formation occur, it will be most active in the area of corrosion, as the latter plays the role of the centre of crystallization. With each cycle of "formation-decay" of gas hydrate, the depth of the corrosion defect increases.

Thus, the mechanism of combined action of corrosive media and gas hydrates is the intensification and localization of corrosion processes. Since the mechanism of corrosion in chloride media is common to both inner pipe and soil corrosion, previously obtained data for soil corrosion were used to more fully describe the process and more correctly establish the general patterns of chloride ion exposure in addition to the results obtained [23, 25, 29-32].

With increasing concentration of chloride ions, the effect of the mechanical factor also increases significantly in the case of general corrosion degradation and for local corrosion. For inner tube corrosion in highly mineralized formation waters (Figs. 9-12) there is a sharp increase in the corrosion rate during the transition from 2.5 mol/l to 3.75 mol/l [23,33].

This corrosion behaviour, in our opinion, is due to the accelerated destruction of passive films by chloride ions when a certain critical concentration is reached. There is an increase in the rate of total and local corrosion for samples aged in gas hydrate compared to control (Figs. 9-12), from the results were calculated the coefficient of influence of gas hydrate on corrosion, which for total corrosion is – 1.13 and for local corrosion – 1.32.

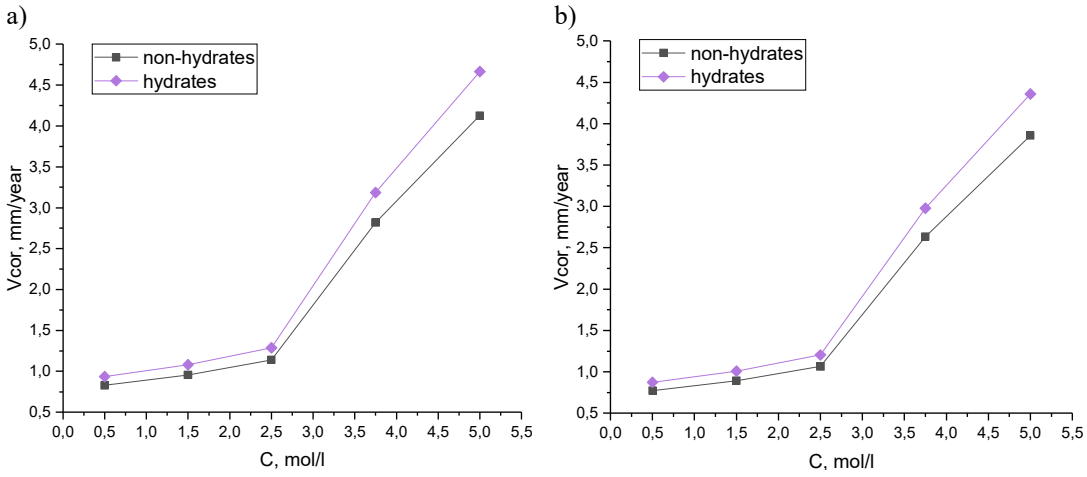

Fig. 9. Inner tube corrosion for 0 MPa (a – St20, b – 17GS)

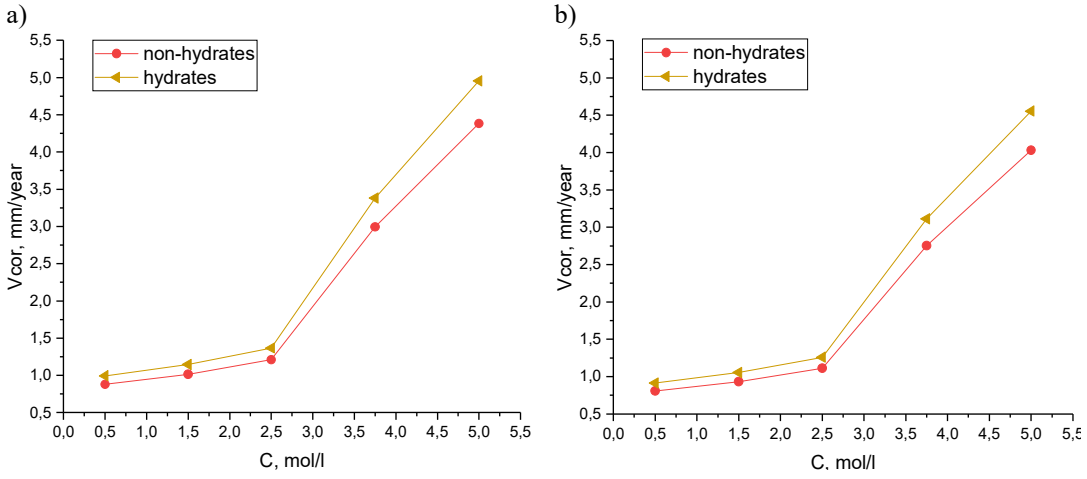

Fig. 10. Inner tube corrosion for 150 MPa (a – St20, b – 17GS)

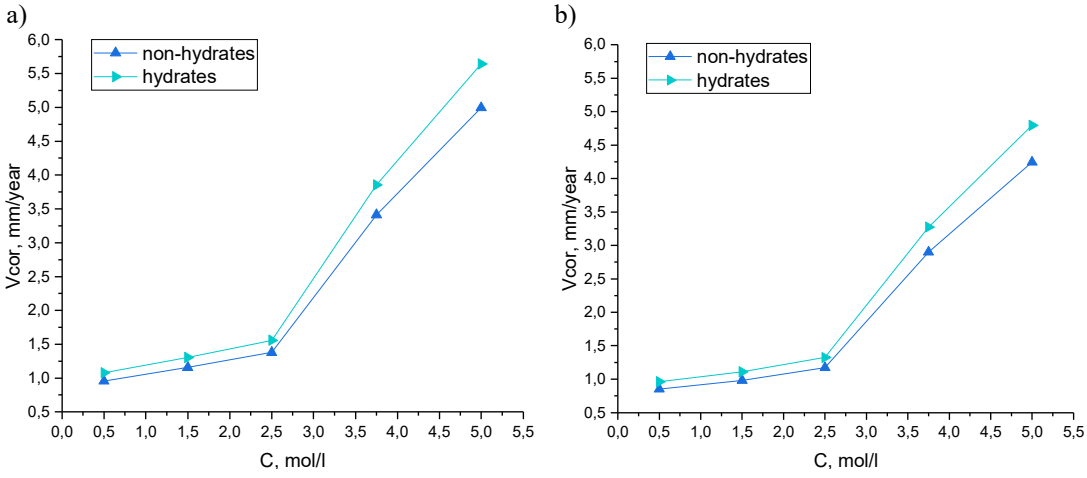

Fig. 11. Inner tube corrosion for 330 MPa (a – St20, b – 17GS)

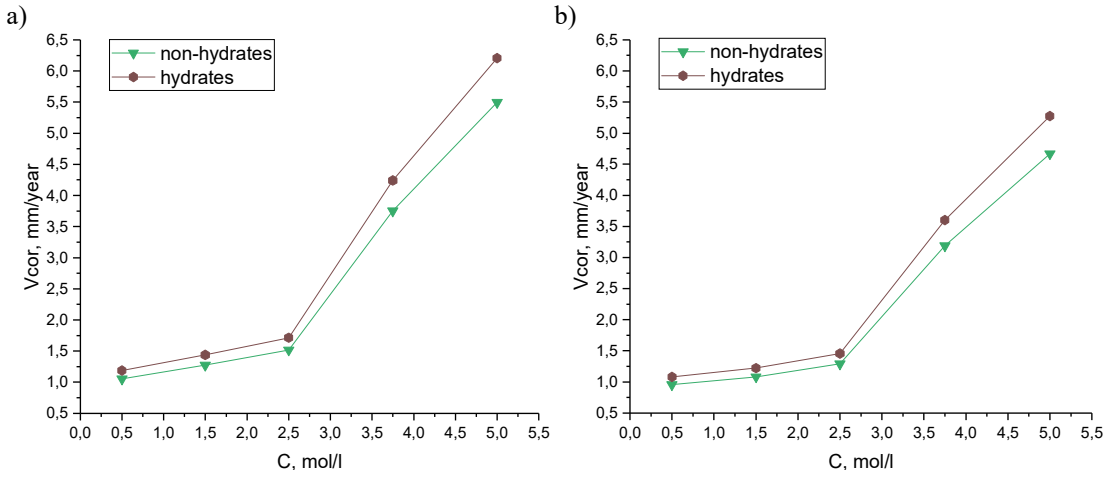

Fig. 12. Inner tube corrosion for 420 MPa (a – St20, b – 17GS)

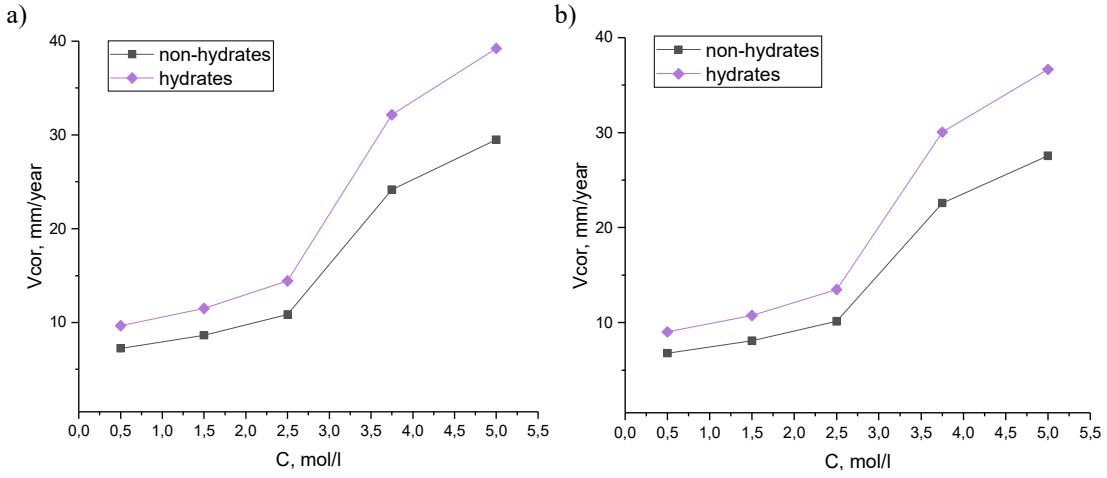

Fig. 13. Inner tube local corrosion for 0 MPa (a – St20, b – 17GS)

The combined analysis of the corrosion behaviour of pipe material in aggressive environments of the chloride type shows similar patterns of the joint influence of the corrosive environment and mechanical factors on the rate of corrosion processes. Thus, for both cases of corrosion considered, we observe the intensification of the influence of the mechanical factor with increasing chloride concentration. In 0.5 mol/l and 1.5 mol/l we see slight changes in the dynamics of the process during the transition from elastic to elastic-plastic zone. In 3.75 mol/l and 5 mol/l, these changes are more pronounced (Figs. 9-12).

With local corrosion with increasing levels of mechanical stresses, we observe a significant intensification of corrosion processes, especially in the area of elastic-plastic deformation (range 1.35 $\sigma^*_{0.2}$ - 1.65 $\sigma^*_{0.2}$ – for 17GS, and 1.45 $\sigma^*_{0.2}$ - 1.8 $\sigma^*_{0.2}$ – for steel 20).

Of particular concern are the indicators of the rate of local corrosion in the simulated formation waters (Figs. 13-16). As well as for a case of uniform corrosion, we fix more intensive action of the mechanical factor at transition from elastic to elastic-plastic deformation.

However, for local corrosion, the strengthening of the role of the mechanical factor is more important. This trend, in our opinion, is associated with the formation of local galvanic cells and the facilitation of the process of dissolving the metal in the tensile zone due to the weakening of the interatomic interaction by increasing the distance between the lattice nodes. In the process of development of local corrosion damage, the concentration of stresses at the bottom of corrosion pits and ulcers also contributes to the strengthening of the role of the mechanical factor.

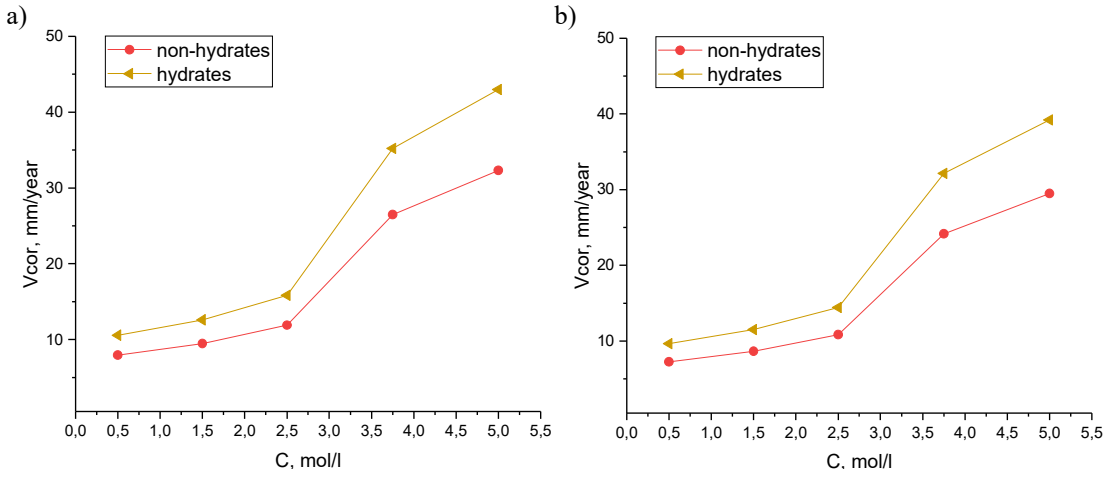

Fig. 14. Inner tube local corrosion for 150 MPa (a – St20, b – 17GS)

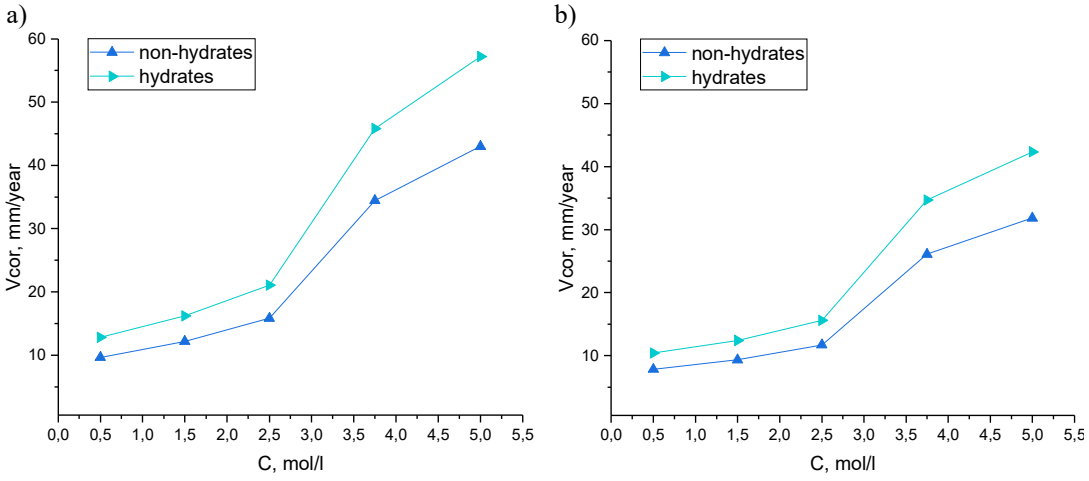

Fig. 15. Inner tube corrosion for 330 MPa (a – St20, b – 17GS)

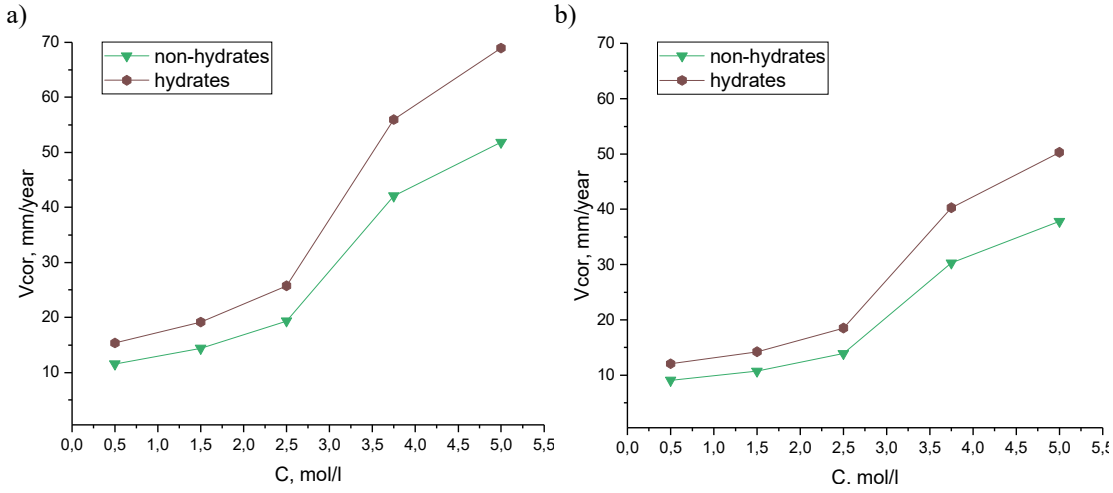

Fig. 16. Inner tube local corrosion for 420 MPa (a – St20, b – 17GS)

Thus, more favourable conditions are created for their growth not in width, but in depth. The second determining factor is the ability of chloride ions to destroy passive films. Due to the effect of this effect, we observe a significant increase in the rate of both local and general corrosion during the transition from 2.5 to 3.75 and 5 mol/l (Figs. 9-16).

To correctly assess the operational risks, resource and residual life of safe operation, it is extremely important to know the rate of thinning of the pipeline wall during operation to prevent possible emergencies in time (Figs. 4-11). We observe similarities to the corresponding dependences in mass losses [31]. It is especially important to analyse groundwater along pipeline routes in order to timely assess the risks of corrosion degradation of pipeline steel, prevent and prevent depressurization or more severe failures and emergencies [34-37]. Increased risks of emergency situations caused by corrosion-mechanical processes will be primarily for discharge lines and other industrial pipelines that are operated without active corrosion protection [38-42].

Depending on the stress level and for the corresponding chloride concentration, the increase in the total corrosion rate due to the action of gas hydrate for steel 17GS is from 0.1 to 0.67 mm/year, for St20 steel from 0.11 to 0.72 mm/year (Figs. 4-7).

For the case of corrosion in formation waters, the jump in corrosion rates during the transition from 2.5 to 3.75 and 5 mol/l is even more obvious. Such a sharp change in performance suggests a change in the patterns of corrosion processes.

For corrosion, taking into account the localization, depending on the stress level and for the corresponding chloride concentration, the increase due to the action of gas hydrate for steel 17GS is from 6.8 to 14.4 mm/year, for St20 steel from 7.3 to 17.1 mm/year (Figs. 13-16).

4. Conclusions

According to the results of visual inspection of the inner surface of the fragments of the discharge lines, a significant localization of corrosion processes was established.

To select the stress levels of corrosion-mechanical tests, the number and geometric dimensions of deep defects were analysed and the effective stress concentration coefficients in the pipe wall were calculated, taking into account which the range is 164-545 MPa. Stress levels of 240, 330, 420 and 510 MPa were selected for the tests.

Corrosion-mechanical tests of samples of pipe steels St20 and 17GS in 5 environments modelling formation waters were carried out. According to the results of corrosion-mechanical tests, the coefficient of influence of gas hydrates K_{hydr} = 1.13 was calculated for general corrosion and K_{hydr} =1.32 for local corrosion.

Acknowledgements

The research presented in this article was performed with the financial support of the National Research Fund of Ukraine (grant number 2020.01/0417).

References

[1] G.A. Olah, Beyond oil and gas: the methanol economy, Angewandte Chemie 44/18 (2005) 2636-2639. DOI: https://doi.org/10.1002/anie.200462121

[2] B.C. Gbaruko, J.C. Igwe, P.N. Gbaruko, R.C. Nwokeoma, Gas hydrates and clathrates: Flow assurance, environmental and economic perspectives and the Nigerian liquified natural gas project, Journal of Petroleum Science and Engineering 56/1-3 (2007) 192-198. DOI: https://doi.org/10.1016/j.petrol.2005.12.011

[3] A.V. Yavorskyi, M.O. Karpash, L.Y. Zhovtulia, L.Y. Poberezhny, P.O. Maruschak, Safe operation of engineering structures in the oil and gas industry, Journal of Natural Gas Science and Engineering 46 (2017) 289-295. DOI: https://doi.org/10.1016/j.jngse.2017.07.026

[4] A. Demirbas, M. Rehan, B.O. Al-Sasi, A.S. Nizami, Evaluation of natural gas hydrates as a future methane source, Petroleum Science and Technology 34/13 (2016) 1204-1210. DOI: https://doi.org/10.1080/10916466.2016.1185442

[5] A.V. Yavorskyi, M.O. Karpash, L.Y. Zhovtulia, L.Y. Poberezhny, P.O. Maruschak, O. Prentkovskis, Risk management of a safe operation of engineering structures in the oil and gas sector, Proceedings of the 20th International Conference "Transport Means 2016", Juodkrantė, Lithuania, 2016, 370-373.

[6] S.A. Aromada, B. Kvamme, New approach for evaluating the risk of hydrate formation during transport of hydrocarbon hydrate formers of sI and sII, AIChE Journal 65/3 (2019) 1097-1110. DOI: https://doi.org/10.1002/aic.16493

[7] J. Zhao, Y. Song, X.L. Lim, W.H. Lam, Opportunities and challenges of gas hydrate policies with consideration of environmental impacts, Renewable and Sustainable Energy Reviews 70 (2017) 875-885. DOI: https://doi.org/10.1016/j.rser.2016.11.269

[8] O. Nashed, B. Partoon, B. Lal, K.M. Sabil, A.M. Shariff, Review the impact of nanoparticles on the thermodynamics and kinetics of gas hydrate formation, Journal of Natural Gas Science and Engineering 55 (2018) 452-465. DOI: https://doi.org/10.1016/j.jngse.2018.05.022

[9] A.O. Oluwatoyin, A.A. Sarah, F.O. Goodness, Development of Thermodynamic Model with Gopal's Constants for the Inhibition of Gas Hydrates Formation in Gas Pipeline, Current Journal of Applied Science and Technology 38/6 (2020) 1-8. DOI: https://doi.org/10.9734/cjast/2019/v38i630441

[10] M.M. Prykhodko, L.Y. Poberezhny, D.V. Kukhtar, V.V. Romaniuk, I.L. Bodnaruk, A.V. Muliar, Forecasting temperature behavior of soil in Gas field exploitation areas. Proceedings of the Conference Geoinformatics: Theoretical and Applied Aspects 2020, Kyiv, Ukraine, 2020, 1-5. DOI: https://doi.org/10.3997/2214-4609.2020geo129

[11] L. Poberezhny, P. Maruschak, A. Hrytsanchuk, L. Poberezhna, O. Prentkovskis, A. Stanetsky, Impact of gas hydrates and long-term operation on fatigue characteristics of pipeline steels, Procedia Engineering 187 (2017) 356-362. DOI: https://doi.org/10.1016/j.proeng.2017.04.386

[12] B. Kvamme, S.A. Aromada, Risk of hydrate formation during the processing and transport of Troll gas from the North Sea, Journal of Chemical and Engineering Data 62/7 (2017) 2163-2177. DOI: https://doi.org/10.1021/acs.jced.7b00256

[13] S.Y. Misyura, I.G. Donskoy, Ways to improve the efficiency of carbon dioxide utilization and gas hydrate storage at low temperatures, Journal of CO_2 Utilization 34 (2019) 313-324. DOI: https://doi.org/10.1016/j.jcou.2019.07.010

[14] P. Maruschak, S. Panin, I. Danyliuk, L. Poberezhnyi, T. Pyrig, R. Bishchak, I. Vlasov, Structural and mechanical defects of materials of offshore and onshore main gas pipelines after long-term operation, Open Engineering 5/1 (2015) 365-372. DOI: https://doi.org/10.1515/eng-2015-0045

[15] L. Poberezhnyi, P. Maruschak, O. Prentkovskis, I. Danyliuk, T. Pyrig, J. Brezinová, Fatigue and failure of steel of offshore gas pipeline after the laying operation, Archives of Civil and Mechanical Engineering 16/3 (2016) 524-536. DOI: https://doi.org/10.1016/j.acme.2016.03.003

[16] V. Bondarenko, I. Kovalevska, D. Astafiev, O. Malova, Examination of phase transition of mine methane to gas hydrates and their sudden failure–Percy Bridgman's effect, Solid State Phenomena 277 (2018) 137-146. DOI: https://doi.org/10.4028/www.scientific.net/SSP.277.137

[17] P. Maruschak, L. Poberezny, O. Prentkovskis, R. Bishchak, A. Sorochak, D. Baran, Physical and mechanical aspects of corrosion damage of distribution gas pipelines after long-term operation, Journal of Failure Analysis and Prevention 18/3 (2018) 562-567. DOI: https://doi.org/10.1007/s11668-018-0439-z

[18] C. Wang, Y. Liu, W. Hou, C. Liu, Y. Zheng, G. Wang, Dynamic Risk Analysis on Offshore Natural Gas Hydrate Production Test Based on DBN-GO Method, Journal of Natural Gas Science and Engineering 91 (2021) 103961. DOI: https://doi.org/10.1016/j.jngse.2021.103961

[19] E.I. Kryzhanivs'Kyi, R.S. Hrabovs'Kyi, I.Y. Fedorovych, R.A. Barna, Evaluation of the Kinetics of Fracture of Elements of a Gas Pipeline after Operation, Materials Science 51/1 (2015) 7-14. DOI: https://doi.org/10.1007/s11003-015-9804-1

[20] E.I. Kryzhanivs'Kyi, R.S. Hrabovs'Kyi, O.Y. Vytyaz', Influence of the geometry of corrosion-fatigue cracks on the residual service life of objects intended for long-term operation, Materials Science 54/5 (2019) 647-655. DOI: https://doi.org/10.1007/s11003-019-00229-8

[21] W.D. Pilkey, D.F. Pilkey, Z. Bi, Peterson's stress concentration factors, John Wiley & Sons, 2020.

[22] T. An, S. Zheng, H. Peng, X. Wen, L. Chen, L. Zhang, Synergistic action of hydrogen and stress concentration on the fatigue properties of X80 pipeline steel, Materials Science and Engineering: A 700 (2017) 321-330. DOI: https://doi.org/10.1016/j.msea.2017.06.029

[23] V.Y. Chernov, V.D. Makarenko, E.I. Kryzhanivs' kyi, L.S. Shlapak, Causes and mechanisms of local corrosion in oil-field pipelines, Materials Science 38/5 (2002) 729-737. DOI: https://doi.org/10.1023/A:1024274726352

[24] H. Neuber, Theory of Stress Concentration for Shear-Strained Prismatical Bodies With Arbitrary Nonlinear Stress-Strain Law, Journal of Applied Mechanics 28/4 (1961) 544-550. DOI: https://doi.org/10.1115/1.3641780

[25] E.I. Kryzhanivs'kyi, I.M. Hoisan, O.Z. Student, Specific Features of the Growth of Fatigue Cracks in 36G2S Steel of Drill Pipes After the Recovery Heat Treatment, Materials Science 50/1 (2014) 92-97. DOI: https://doi.org/10.1007/s11003-014-9695-6

[26] Ya. Doroshenko, V. Zapukhliak, Ya. Grudz, L. Poberezhny, A. Hrytsanchuk, P. Popovych, O. Shevchuk, Numerical simulation of the stress state of an erosion-worn tee of the main gas pipeline, Archives

of Materials Science and Engineering 101/2 (2020) 63-78. DOI: https://doi.org/10.5604/01.3001.0014.1192
[27] P. Popovych, O. Shevchuk, V. Dzyura, L. Poberezhna, V. Dozorskyy, A. Hrytsanchuk, Assessment of the influence of corrosive aggressive cargo transportation on vehicle reliability, International Journal of Engineering Research in Africa 38 (2018) 17-25. DOI: https://doi.org/10.4028/www.scientific.net/JERA.38.17
[28] O. Mandryk, A. Pukish, A. Zelmanovych, Formation peculiarities of physical and chemical composition of highly mineralized edge water, Mining of Mineral Deposits 11/1 (2017) 72-79. DOI: https://doi.org/10.15407/mining11.01.072
[29] L. Poberezhny, I. Chudyk, A. Hrytsanchuk, O. Mandryk, T. Kalyn, H. Hrytsuliak, Y. Yakymechko, Influence of Hydrate Formation and Concentration of Salts on the Corrosion of Steel 20 Pipelines, Management Systems in Production Engineering 28/3 (2020) 141-147. DOI: https://doi.org/10.2478/mspe-2020-0021
[30] Y. Song, G. Jiang, Y. Chen, P. Zhao, Y. Tian, Effects of chloride ions on corrosion of ductile iron and carbon steel in soil environments, Scientific Reports 7/1 (2017) 6865. DOI: https://doi.org/10.1038/s41598-017-07245-1
[31] L.Y. Pobereznyi, L.Y. Poberezhna, P.O. Maruschak, S.V. Panin, Assessment of Potential Environmental Risks from Saline Soils Subsidence, IOP Conference Series: Earth and Environmental Science 50/1 (2017) 012046. DOI: https://doi.org/10.1088/1755-1315/50/1/012046
[32] Z. Mahidashti, M. Rezaei, M.P. Asfia, Internal under-deposit corrosion of X60 pipeline steel upon installation in a chloride-containing soil environment, Colloids and Surfaces A: Physicochemical and Engineering Aspects 602 (2020) 125120. DOI: https://doi.org/10.1016/j.colsurfa.2020.125120
[33] R.A. Barna, P.V. Popovych, Influence of Operating Media on the Fatigue Fracture of Steels for Elements of Agricultural Machines, Materials Science 50 (2014) 377-380. DOI: https://doi.org/10.1007/s11003-014-9729-0
[34] F. Yu, S. Xue, Y. Zhao, G. Chen, Risk assessment of oil spills in the Chinese Bohai Sea for prevention and readiness, Marine Pollution Bulletin 135 (2018) 915-922. DOI: https://doi.org/10.1016/j.marpolbul.2018.07.029
[35] I. Chudyk, L. Poberezhny, A. Hrysanchuk, L. Poberezhna, Corrosion of drill pipes in high mineralized produced waters, Procedia Structural Integrity 16 (2019) 260-264. DOI: https://doi.org/10.1016/j.prostr.2019.07.050
[36] L.Y. Poberezhnyi, P.O. Marushchak, A.P. Sorochak, D. Draganovska, A.V. Hrytsanchuk, B.V. Mishchuk, Corrosive and mechanical degradation of pipelines in acid soils, Strength of Materials 49/4 (2017) 539-549. DOI: https://doi.org/10.1007/s11223-017-9897-x
[37] L. Poberezhny, A. Hrytsanchuk, G. Hrytsuliak, L. Poberezhna, M. Kosmii, Influence of hydrate formation and wall shear stress on the corrosion rate of industrial pipeline materials, Koroze a Ochrana Materialu 62/4 (2018) 121-128. DOI: https://doi.org/10.2478/kom-2018-0017
[38] V. Yuzevych, F. Horbonos, R. Rogalskyi, I. Yemchenko, M. Yasinskyi, Determination of the Place Depressurization of Underground Pipelines in the Monitoring of Oil and Gas Enterprises, International Journal of Recent Technology and Engineering 9/1 (2020) 2274-2281.
[39] L. Poberezhny, A. Hrytsanchuk, I. Okipnyi, L. Poberezhna, A. Stanetsky, N. Fedchyshyn, Minimizing losses during natural gas transportation, Strojnícky Časopis – Journal of Mechanical Engineering 69/1 (2019) 97-108. DOI: https://doi.org/10.2478/scjme-2019-0008
[40] E. Heaver, Internal Stress Corrosion Cracking of Shale Gas Flowlines, Materials Performance, 2020. Available from: https://www.materialsperformance.com/articles/chemical-treatment/2017/11/internal-stress-corrosion-cracking-of-shale-gas-flowlines
[41] V. Zapukhliak, L. Poberezhny, P. Maruschak, V. Grudz Jr, R. Stasiuk, J. Brezinová, A. Guzanová, Mathematical modeling of unsteady gas transmission system operating conditions under insufficient loading, Energies 12/7 (2019) 1325. DOI: https://doi.org/10.3390/en12071325
[42] S. Shin, G. Lee, U. Ahmed, Y. Lee, J. Na, C. Han, Risk-based underground pipeline safety management considering corrosion effect, Journal of Hazardous Materials 342 (2018) 279-289. DOI: https://doi.org/10.1016/j.jhazmat.2017.08.029